Proceedings of Machine Learning Research vol 211:1–13, 2023 5th Annual Conference on Learning for Dynamics and Control

Data-driven Stochastic Output-Feedback Predictive Control: Recursive Feasibility through Interpolated Initial Conditions

Guanru Pan GUANRU.PAN@TU-DORTMUND.DE
Ruchuan Ou RUCHUAN.OU@TU-DORTMUND.DE
Timm Faulwasser TIMM.FAULWASSER@IEEE.ORG
Institute for Energy Systems, Energy Efficiency and Energy Economics,
TU Dortmund University, Dortmund, 44227 Germany

Editors: N. Matni, M. Morari, G. J. Pappas

Abstract

This paper investigates data-driven output-feedback predictive control of linear systems subject to stochastic disturbances. The scheme relies on the recursive solution of a suitable data-driven reformulation of a stochastic Optimal Control Problem (OCP), which allows for forward prediction and optimization of statistical distributions of inputs and outputs. Our approach avoids the use of parametric system models. Instead it is based on previously recorded data and on a recently proposed stochastic variant of Willems' fundamental lemma. The stochastic variant of the lemma is applicable to linear dynamics subject to a large class of stochastic disturbances of Gaussian or non-Gaussian nature. To ensure recursive feasibility, the initial condition of the OCP—which consists of information about past inputs and outputs—is considered as an extra decision variable of the OCP. We provide sufficient conditions for recursive feasibility of the proposed scheme as well as a bound on the asymptotic average performance. Finally, a numerical example illustrates the efficacy and the closed-loop properties of the proposed scheme.

Keywords: Data-driven control, stochastic predictive control, Willems' fundamental lemma

1. Introduction

Data-driven control based on the so-called fundamental lemma by Willems et al. (2005) has attracted a lot of research interest, see Markovsky and Dörfler (2021); De Persis and Tesi (2020) for recent reviews. The pivotal insight of the fundamental lemma is that any controllable LTI system can be characterized by its recorded input-output trajectories provided a persistency of excitation condition to be satisfied. In the context of predictive control this implies that the prediction of future input and output trajectories can be done based on measurements of past trajectories thus alleviating the need for system identification and state estimator design (Yang and Li, 2015; Coulson et al., 2019; Lian and Jones, 2021; Allibhoy and Cortes, 2020). Hence data-driven predictive control schemes are considered for different applications, e.g. (Carlet et al., 2023; Bilgic et al., 2022; Wang et al., 2022a). Rigorous guarantees for closed-loop properties are provided by Berberich et al. (2020, 2021); Bongard et al. (2023) for data-driven predictive control schemes with respect to deterministic LTI systems subjected to noisy measurements.

However, besides measurement noise, so far little has been done on data-driven predictive control for LTI systems subject to stochastic disturbances. One key challenge is the prediction of the future evolution of statistical distributions of the inputs (respectively input policies) and outputs in a data-driven fashion. One approach is to predict the expected value of the future trajectory by the fundamental lemma while handling the stochastic uncertainties offline by probabilistic constraint tightening (Kerz et al., 2021) or directly omitting the stochastic uncertainties in the prediction (Wang et al., 2022b). Alternatively, leveraging the framework of Polynomial Chaos Expansions (PCEs) (Sullivan, 2015) a stochastic variant of Willems' fundamental lemma has been proposed (Pan et al., 2022b). It allows to predict future statistical distributions of inputs and outputs via previously recorded data and knowledge about the distribution of the disturbance.

Extending the conceptual ideas of Pan et al. (2022b) towards stochastic data-driven predictive control with guarantees, Pan et al. (2022c) present first results in a state-feedback setting, while the output-feedback case is discussed by Pan et al. (2022a). Therein, sufficient conditions for recursive feasibility and a bound on the asymptotic average performance are provided by a data-driven design of terminal ingredients and a selection strategy of the initial condition which is similar to the model-based approach of Farina et al. (2013, 2015). The selection of initial conditions considers a binary choice: the current measured value or its predicted value based on the last optimal solution.

In this paper, we extend the data-driven stochastic output-feedback predictive scheme proposed by Pan et al. (2022a) with an improved initialization strategy. Instead of the binary selection strategy described above, the proposed scheme interpolates between the measured value and the latest prediction in a continuous fashion. In model-based stochastic predictive control this has been considered by Köhler and Zeilinger (2022); Schlüter and Allgöwer (2022); while an alternative initialization strategy is considered by Korda et al. (2011). The main contribution of the present paper are sufficient conditions for recursive feasibility and a bound on the asymptotic average performance of the proposed data-driven stochastic output-feedback scheme.

2. Problem statement and preliminaries

We investigate a stochastic output feedback approach to control LTI systems with unknown system matrices. Hence, we first detail the considered setting, then we recall the representation of $\mathcal{L}^2$ random variables via polynomial chaos, before we arrive at the stochastic fundamental lemma.

2.1. Considered system class

We consider stochastic LTI systems in AutoRegressive with eXtra input (ARX) form

$$Y_k = \Phi Z_k + DU_k + W_k, \quad Z_0 = Z_{\text{ini}}, \tag{1}$$

with input $U_k \in \mathcal{L}^2(\Omega, \mathcal{F}, \mu; \mathbb{R}^{n_u})$, output $Y_k \in \mathcal{L}^2(\Omega, \mathcal{F}, \mu; \mathbb{R}^{n_y})$, disturbance $W_k \in \mathcal{L}^2(\Omega, \mathcal{F}, \mu; \mathbb{R}^{n_w})$ ($n_w = n_y$), and extended state

$$Z_k \doteq \begin{bmatrix} \mathbf{U}_{[k-T_{\text{ini}},k-1]} \\ \mathbf{Y}_{[k-T_{\text{ini}},k-1]} \end{bmatrix} = \begin{bmatrix} U_{k-T_{\text{ini}}}^\top, U_{k-T_{\text{ini}}+1}^\top, \cdots, U_{k-1}^\top, Y_{k-T_{\text{ini}}}^\top, \cdots, Y_{k-1}^\top \end{bmatrix}^\top \in \mathcal{L}^2(\Omega, \mathcal{F}, \mu; \mathbb{R}^{n_z}),$$

with $n_z = T_{\text{ini}}(n_u + n_y)$ which contains last T_{ini} inputs and outputs.

Here, Ω denotes the sample space, $\mathcal{F}$ is a σ algebra, and μ is the considered probability measure. With the specification of the underlying probability space $(\Omega, \mathcal{F}, \mu)$ to be $\mathcal{L}^2$, we restrict the consideration to random variables with finite expectation and finite (co)-variance. Throughout this paper, the system matrices $\Phi \in \mathbb{R}^{n_y \times n_z}$ and $D \in \mathbb{R}^{n_y \times n_u}$ are considered to be unknown, while the statistical distributions of initial condition Z_{ini} and disturbances $\{W_k\}_{k\in\mathbb{N}}$ are supposed to be known. Furthermore, we consider that all $\{W_k\}_{k\in\mathbb{N}}$ are identical independently distributed ($i.i.d.$) with zero mean and finite co-variance, i.e., we assume for all $k \in \mathbb{N}$, $\mathbb{E}[W_k] = 0$ and $\Sigma[W_k] = \Sigma_W$. We remark that the initial condition and the disturbances are not restricted to be Gaussian.

For a specific uncertainty outcome $\omega \in \Omega$, we denote the realization of W_k as $w_k \doteq W_k(\omega)$. Likewise, the input, output, and extended state realizations are written as $u_k \doteq U_k(\omega)$, $y_k \doteq Y_k(\omega)$, and $z_k \doteq Z_k(\omega)$, respectively. Moreover, given z_{ini} and w_k, $k \in \mathbb{N}$, the stochastic system (1) induces the *realization dynamics*

$$y_k = \Phi z_k + Du_k + w_k, \quad z_0 = z_{\text{ini}}. \tag{2}$$

Throughout the paper, we assume the input, output, and disturbance realizations u_k, y_k, and w_{k-1} to be measured at time instant k. For the case of unmeasured disturbances, we refer to the disturbance estimation schemes tailored to ARX models, see (Pan et al., 2022b; Wang et al., 2022b) .

Assumption 1 *There exists a minimal state-space representation*

$$X_{k+1} = AX_k + BU_k + EW_k, \quad X_0 = X_{ini}, \quad Y_k = CX_k + DU_k + W_k, \tag{3}$$

with (A, B) controllable and (A, C) observable such that for some initial condition X_{ini} and W_k, $k \in \mathbb{N}$, the input-output trajectories of (1) and (3) coincide.

For insights into the problem of mapping a ARX model to its minimal state-space representations, see Sadamoto (2022); Wu (2022). Moreover, consider Z_k as state, one—not necessarily minimal—state-space realization of the ARX model (1) is given by

$$Z_{k+1} = \widetilde{A}X_k + \widetilde{B}U_k + \widetilde{E}W_k, \quad Z_0 = Z_{\text{ini}}, \quad Y_k = \Phi X_k + DU_k + W_k, \tag{4}$$

with

$$\widetilde{A} = \left[\begin{array}{cccc} 0 & I_{(T_{\text{ini}}-1)n_u} & 0 & 0 \\ 0_{n_u\times n_u} & 0 & 0_{n_u\times n_y} & 0 \\ 0 & 0 & 0 & I_{(T_{\text{ini}}-1)n_y} \\ \hline \multicolumn{4}{c}{\Phi} \end{array}\right], \quad \widetilde{B} = \left[\begin{array}{c} 0 \\ I_{n_u} \\ 0 \\ \hline D \end{array}\right], \quad \widetilde{E} = \begin{bmatrix} 0 \\ I_{n_y} \end{bmatrix}.$$

Note that due to Assumption 1 the pair $(\tilde{A}, \tilde{B})$ is stabilizable (Bongard et al., 2023).

2.2. Representation of random variables via polynomial chaos expansions

It is well-known that for stochastic LTI systems subject to Gaussian disturbances, the evolution of statistical distributions of inputs (generated via affine policies) and outputs can be exactly represented by the first two moments, cf. Farina et al. (2013, 2015). However, this is not necessarily the case for non-Gaussian disturbances. Moreover, observe that already in a Gaussian setting moments constitute non-linear representations of random variables as any scalar Gaussian is given by the sum of its mean with its standard deviation (= square root of variance) times a standard normal-distributed random variable. Alternatively, one could rely on scenario-based approaches and sampling strategies (Kantas et al., 2009; Tempo et al., 2013; Schildbach et al., 2014). However, this induces substantial computational effort.

Alternatively, we employ Polynomial Chaos Expansions (PCE) to provide a tractable linear surrogate of (1) by representing $\mathcal{L}^2$ random variables in a suitable polynomial basis. PCE dates back to Wiener (1938), and we refer to Sullivan (2015) for a general introduction, see, e.g., (Paulson et al., 2014; Mesbah et al., 2014; Ou et al., 2021) for applications in control.

Consider an orthogonal polynomial basis $\{\phi^j\}_{j=0}^{\infty}$ which spans $\mathcal{L}^2(\Omega, \mathcal{F}, \mu; \mathbb{R})$, i.e., $\langle \phi^i, \phi^j \rangle \doteq \int_\Omega \phi^i(\omega)\phi^j(\omega)\,\mathrm{d}\mu(\omega) = \delta^{ij}\|\phi^j\|^2$, where δ^{ij} is the Kronecker delta and $\|V\| \doteq \sqrt{\langle V, V\rangle}$ is the $\mathcal{L}^2$ norm of $V \in \mathcal{L}^2(\Omega, \mathcal{F}, \mu; \mathbb{R})$. With respect to the basis $\{\phi^j\}_{j=0}^{\infty}$, a real-valued random scalar variable $V \in \mathcal{L}^2(\Omega, \mathcal{F}, \mu; \mathbb{R})$ can be expressed as $V = \sum_{j=0}^{\infty} \mathsf{v}^j \phi^j$ with $\mathsf{v}^j = \langle V, \phi^j \rangle / \|\phi^j\|^2$, where $\mathsf{v}^j \in \mathbb{R}$ is called the j-th PCE coefficient. For a vector-valued random variable $V \in \mathcal{L}^2(\Omega, \mathcal{F}, \mu; \mathbb{R}^{n_v})$, applying PCE component-wise, the j-th coefficient is given as $\mathsf{v}^j = [\mathsf{v}^{1,j}\ \mathsf{v}^{2,j}\ \cdots\ \mathsf{v}^{n_v,j}]^\top$ with $\mathsf{v}^{i,j}$ as the j-th PCE coefficient of the component V^i of V.

In practice one often terminates the PCE series after a finite number of terms for more efficient computation. However, this may lead to truncation errors (Mühlpfordt et al., 2018). Fortunately, random variables that follow some widely-used distributions admit exact finite-dimensional PCEs with only two terms in suitable polynomial bases, see (Koekoek and Swarttouw, 1998; Xiu and Karniadakis, 2002). For example, the Legendre basis is preferably chosen for uniformly-distributed random variables and Hermite polynomials are used for Gaussians.

Definition 1 (Exact PCE representation (Mühlpfordt et al., 2018)) *The PCE of a random variable $V \in \mathcal{L}^2(\Omega, \mathcal{F}, \mu; \mathbb{R}^{n_v})$ is said to be exact with dimension L if $V - \sum_{j=0}^{L-1} \mathsf{v}^j \phi^j = 0$.*

Notice that with an exact PCE of finite dimension, the expected value, variance, and covariance of $V \in \mathcal{L}^2(\Omega, \mathcal{F}, \mu; \mathbb{R}^{n_v})$ can be efficiently calculated from its PCE coefficients

$$\mathbb{E}[V] = \mathsf{v}^0, \quad \mathbb{V}[V] = \sum_{j=1}^{L-1} (\mathsf{v}^j)^2 \|\phi^j\|^2, \quad \Sigma[V] = \sum_{j=1}^{L-1} \mathsf{v}^j \mathsf{v}^{j\top} \|\phi^j\|^2, \tag{5}$$

where $(\mathsf{v}^j)^2 \doteq \mathsf{v}^j \circ \mathsf{v}^j$ denotes the Hadamard product (Lefebvre, 2021). Finally, observe that (finite or infinite) PCEs of $\mathcal{L}^2$ random variables constitute linear representations of random variables.

To the end of reformulation of (1) with finite dimensional PCEs, we assume that Z_{ini} and W_k, $k \in \mathbb{N}^+$ admit exact PCEs in the basis $\{\phi_{\text{ini}}^j\}_{j=0}^{L_{\text{ini}}-1}$, respectively, in the basis $\{\varphi_k^j\}_{j=0}^{L_w-1}$. Consider system (1) for a finite horizon $N \in \mathbb{N}$ and the finite-dimensional joint basis

$$\{\phi^j\}_{j=0}^{L-1} = \left\{1, \{\phi_{\text{ini}}^j\}_{j=1}^{L_{\text{ini}}-1}, \bigcup_{i=0}^{N-1} \{\varphi_i^j\}_{j=1}^{L_w-1}\right\}, \qquad L = L_{\text{ini}} + N(L_w - 1) \in \mathbb{N}^+. \tag{6}$$

Then, for all $k \in \mathbb{I}_{[0,N-1]}$, U_k, Y_k, and thus Z_k also admit exact PCEs in the chosen basis if U_k is determined from an affine function of the extended state Z_k, cf. the formal proofs given in (Pan et al., 2022a,b). Note that the key aspect of $\{\phi^j\}_{j=0}^{L-1}$ is that it is the union of the bases for Z_{ini} and W_k, $k \in \mathbb{I}_{[0,N-1]}$. Thus, PCE enables uncertainty propagation over any finite prediction horizon.

Replacing all random variables in (1) with their PCE representation in the basis $\{\phi^j\}_{j=0}^{L-1}$ and projecting onto the basis functions ϕ^j, we obtain the dynamics of the PCE coefficients. For given $\mathsf{z}_{\text{ini}}^j$ and w_k^j, $k \in \mathbb{N}$, the *dynamics of the PCE coefficients* read

$$\mathsf{y}_k^j = \Phi \mathsf{z}_k^j + D\mathsf{u}_k^j + \mathsf{w}_k^j, \quad \mathsf{z}_0^j = \mathsf{z}_{\text{ini}}^j, \quad j \in \mathbb{I}_{[0,L-1]}. \tag{7}$$

2.3. Data-driven system representation via a stochastic fundamental lemma

It is the linearity of the series expansion which ensures that the original stochastic system (1) and its PCE formulation (7) are structurally similar. Subsequently, we recall a stochastic variant of Willems' fundamental lemma which exploits this structural similarity.

Definition 2 (Persistency of excitation (Willems et al., 2005)) *Let $T, t \in \mathbb{N}^+$. An input sequence $\mathbf{u}_{[0,T-1]}$ is said to be persistently exciting of order t if the Hankel matrix* $\mathcal{H}_t(\mathbf{u}_{[0,T-1]}) \doteq \begin{bmatrix} u_0 & \cdots & u_{T-t} \\ \vdots & \ddots & \vdots \\ u_{t-1} & \cdots & u_{T-1} \end{bmatrix}$ *is of full row rank.*

Lemma 3 (Lem. 4, Cor. 2 (Pan et al., 2022b)) *Let Assumption 1 hold. Consider system (1) and a T-length realization trajectory tuple $(\mathbf{u}, \mathbf{w}, \mathbf{y})_{[0,T-1]}$ of its corresponding realization dynamics (2). Let $(\mathbf{u}, \mathbf{w})_{[0,T-1]}$ be persistently exciting of order $n_x + t$. Then $(\mathbf{U}, \mathbf{W}, \mathbf{Y})_{[0,t-1]}$ is a trajectory of (7) if and only if there exists $G \in \mathcal{L}^2(\Omega, \mathcal{F}, \mu; \mathbb{R}^{T-t+1})$ such that $\mathcal{H}_t(\mathbf{v}_{[0,T-1]})G = \widetilde{\mathbf{V}}_{[0,t-1]}$ holds for all $(\mathbf{v}, \mathbf{V}) \in \{(\mathbf{u}, \mathbf{U}), (\mathbf{w}, \mathbf{W}), (\mathbf{y}, \mathbf{Y})\}$.*

Moreover, $(\mathsf{u}, \mathsf{w}, \mathsf{y})^j_{[0,t-1]}$, $j \in \mathbb{I}_{[0,L-1]}$ is a trajectory of the dynamics of PCE coefficients (7) if and only if there exists $\mathsf{g}^j \in \mathbb{R}^{T-t+1}$ such that $\mathcal{H}_t(\mathbf{v}_{[0,T-1]})\mathsf{g}^j = \mathsf{v}^j_{[0,t-1]}$, $j \in \mathbb{I}_{[0,L-1]}$, holds for all $(\mathbf{v}, \mathsf{v}) \in \{(\mathbf{u}, \mathsf{u}), (\mathbf{w}, \mathsf{w}), (\mathbf{y}, \mathsf{y})\}$. □

As the page limit prohibits the detailed discussion of the above we refer to Pan et al. (2022b); Faulwasser et al. (2023) for proofs and examples. However, the key insight underlying the above results is that the dynamics of random variables (1), its realization dynamics (2), and the dynamics of PCE coefficients (7) share the same system structure and matrices. Hence, their finite-length trajectories can be linked to the trajectories of realization dynamics (2) as shown in Lemma 3. Put differently, in Lemma 3 *Hankel matrices in measured realization data* are used to predict the future evolution of random variables.

3. Data-driven stochastic output-feedback predictive control

In this section, we extend the data-driven stochastic output-feedback predictive control by Pan et al. (2022a) through interpolation of the initial condition. We provide sufficient conditions for recursive feasibility and a bound on the asymptotic average performance of the extended scheme.

3.1. Data-driven stochastic OCP with interpolated initial conditions

Consider the stochastic LTI system (1), its realization dynamics (2), and its PCE coefficients dynamics (7) with respect to the basis $\{\phi^j\}_{j=0}^{L-1}$, cf. (6). Suppose that a realization trajectory $(\mathbf{u}, \mathbf{w}, \mathbf{y})_{[0,T-1]}$ of (2) is available with $(\mathbf{u}, \mathbf{w})_{[0,T-1]}$ persistently exciting of order $n_x + N + T_{\text{ini}}$.

In the following, consider $\mathsf{v} \doteq [\mathsf{v}^{0\top}, \mathsf{v}^{1\top}, \dots, \mathsf{v}^{L-1\top}]^\top$ as the vectorization of PCE coefficients over PCE dimensions, and let $\mathsf{v}^j_{i|k}$ be the predicted value of v^j_{k+i} at time instant k, $\mathsf{v} \in \{\mathsf{u}, \mathsf{y}, \mathsf{z}\}$. At time instant $k \in \mathbb{N}$, given the PCE coefficients of the disturbances, i.e. w_{k+i}, $i \in \mathbb{I}_{[0,N-1]}$, the realization of the current extended state z_k, and the predicted PCE coefficients from last step $\mathsf{z}^\star_{1|k-1}$, we consider the following data-driven stochastic OCP

$$V_N\left(z_k, \mathsf{z}^\star_{1|k-1}\right) \doteq \min_{(\mathsf{u},\mathsf{y},\mathsf{z})^\cdot_{\cdot|k}, \mathsf{g}^\cdot, \mu} \sum_{j=0}^{L-1} \|\phi^j\|^2 \left(\sum_{i=0}^{N-1} \left(\|\mathsf{y}^j_{i|k}\|^2_Q + \|\mathsf{u}^j_{i|k}\|^2_R \right) + \|\mathsf{z}^j_{N|k}\|^2_P \right) \tag{8a}$$

$$\text{subject to} \quad \begin{bmatrix} \mathcal{H}_{N+T_{\text{ini}}}(\mathbf{u}_{[0,T-1]}) \\ \mathcal{H}_{N+T_{\text{ini}}}(\mathbf{y}_{[0,T-1]}) \\ \mathcal{H}_N(\mathbf{w}_{[T_{\text{ini}},T-1]}) \end{bmatrix} \mathsf{g}^j = \begin{bmatrix} \mathsf{u}^j_{[-T_{\text{ini}},N-1]|k} \\ \mathsf{y}^j_{[-T_{\text{ini}},N-1]|k} \\ \mathsf{w}^j_{[k,k+N-1]} \end{bmatrix}, \quad \forall j \in \mathbb{I}_{[0,L-1]} \tag{8b}$$

$$\mathsf{z}_{0|k} \in \mathbb{Z}_{\text{ini}}\left(\mu, z_k, \mathsf{z}^\star_{1|k-1}\right) \tag{8c}$$

$$\mathsf{u}^0_{i|k} \pm \sigma(\varepsilon_u)\sqrt{\textstyle\sum_{j=1}^{L-1}(\mathsf{u}^j)^2\langle\phi^j\rangle^2} \in \mathbb{U},\ \mathsf{y}^0_{i|k} \pm \sigma(\varepsilon_y)\sqrt{\textstyle\sum_{j=1}^{L-1}(\mathsf{y}^j)^2\langle\phi^j\rangle^2} \in \mathbb{Y},\ \forall i \in \mathbb{I}_{[0,N-1]} \tag{8d}$$

$$\mathsf{u}^{j'}_{i|k} = 0, \quad \forall j' \in \mathbb{I}_{[L_{\text{ini}}+i(L_w-1),L-1]}, \quad \forall i \in \mathbb{I}_{[0,N-1]}, \tag{8e}$$

$$\mathsf{z}^0_{N|k} \in \mathbb{Z}_{\text{f}}, \quad \textstyle\sum_{j=1}^{L-1} \mathsf{z}^{j\top}_{N|k}\Gamma \mathsf{z}^j_{N|k}\|\phi^j\|^2 \leq \gamma, \tag{8f}$$

$$\mathsf{z}^j_{i|k} = \left[\mathsf{u}^{j\top}_{[i-T_{\text{ini}},i-1]|k}, \mathsf{y}^{j\top}_{[i-T_{\text{ini}},i-1]|k}\right]^\top, \quad i \in \mathbb{I}_{[0,N]}, \quad j \in \mathbb{I}_{[0,L-1]}. \tag{8g}$$

Observe that the decision variables z are redundant. They are introduced for the sake of compact notation and they can easily be avoided via (8g). The objective function (8a) penalizes the predicted input and output PCE coefficients with $R = R^\top \succ 0$ and $Q = Q^\top \succ 0$. Moreover, $P = P^\top \succ 0$ characterizes the terminal cost with respect to the PCE coefficients $\mathsf{z}^j_{N|k}$. Formulated in terms of PCE coefficients, the objective function (8a) is equivalent to the expected value of its counterpart with random variables (Pan et al., 2022b). The linear equalities (8b)–(8c) encode the dynamics of the PCE coefficients (7) in a non-parametric fashion and based on measured data, cf. Lemma 3.

Furthermore, (8d) is a usually conservative approximation of chance constraints with $\sigma(\varepsilon_v) = \sqrt{(2-\varepsilon_v)/\varepsilon_v}$, $v \in \{u, y\}$ (Farina et al., 2013). The required probabilities are indicated by $1-\varepsilon_u$ and $1-\varepsilon_y$. Causality is ensured in (8e) by specifying the PCE coefficients of $U_{i|k}$ to be zero if they correspond to the non-past disturbances $W_{i'}$, $i' \geq i$. The terminal constraints are specified in (8f). Specifically, considering $Z_{N|k} \doteq \sum_{j=0}^{L-1} \mathsf{z}^j_{N|k}\phi^j$, the terminal constraints (8f) require the expected value of $Z_{N|k}$ to be inside of the terminal region $\mathbb{Z}_\text{f}$ and the trace of its covariance weighted by Γ to be smaller than $\gamma \in R^+$. Precisely, the terminal ingredients satisfy the following assumption.

Assumption 2 (Terminal ingredients (Pan et al., 2022a)) *Consider system (4) given by the matrices $\widetilde{A}$, $\widetilde{B}$, and $\widetilde{E}$. There exist matrices $P = P^\top \succ 0 \in \mathbb{R}^{n_z \times n_z}$, $\Gamma = \Gamma^\top \succ 0 \in \mathbb{R}^{n_z \times n_z}$, $K \in \mathbb{R}^{n_u \times n_z}$ and a positive real number $\gamma \in \mathbb{R}^+$ such that $A_K = \widetilde{A} + \widetilde{B}K$ is Schur, $A_K^\top P A_K - P = -K^\top RK - A_K^\top \widetilde{E}Q\widetilde{E}^\top A_K$, $A_K^\top \Gamma A_K - \Gamma = -I_{n_z}$, and $\gamma = \lambda_{max}(\Gamma)\cdot \operatorname{trace}\left(\Sigma_W \widetilde{E}^\top \Gamma \widetilde{E}\right)$. Moreover, there exists a set $\mathbb{Z}_f \subseteq \mathbb{U}^{T_{ini}} \times \mathbb{Y}^{T_{ini}}$ such that for all $\mathsf{z}^{[0,L-1]}$ satisfying (8f), we have $A_K\mathsf{z}^0 \in \mathbb{Z}_f$, $K\mathsf{z}^0 + \sigma(\varepsilon_u)\sqrt{\sum_{j=1}^{L-1}(K\mathsf{z}^j)^2\|\phi^j\|^2} \in \mathbb{U}$, and $\widetilde{E}^\top A_K\mathsf{z}^0 + \sigma(\varepsilon_y)\sqrt{\sum_{j=1}^{L-1}(\widetilde{E}^\top A_K\mathsf{z}^j)^2\|\phi^j\|^2 + \mathbb{V}[W]} \in \mathbb{Y}$.*

For more details on the data-driven design of the terminal ingredients, we refer to the discussions by Pan et al. (2022a).

The initial condition of OCP (8) is considered in (8c). Given $\mathsf{z}^\star_{1|k-1}$ as the predicted value of z^j_k with respect to the optimal solution at time instant $k-1$, we specify the constraint set in (8c) as

$$\mathbb{Z}_{\text{ini}}\left(\mu, z_k, \mathsf{z}^\star_{1|k-1}\right) \doteq \left\{ \mathsf{z}_{0|k} \;\middle|\; \begin{array}{c} \mathsf{z}^0_{0|k} = \mu z_k + (1-\mu)\mathsf{z}^{0,\star}_{1|k-1}, \quad 0 \leq \mu \leq 1 \\ \displaystyle\sum_{j=1}^{L_{\text{ini}}-1} \mathsf{z}^j_{0|k}\mathsf{z}^{j\top}_{0|k}\|\phi^j\|^2 = (1-\mu)^2 \sum_{j=1}^{L-1} \mathsf{z}^{j,\star}_{1|k-1}\mathsf{z}^{j,\star\top}_{1|k-1}\|\phi^j\|^2 \\ \mathsf{z}^j_{0|k} = 0, \quad j = \mathbb{I}_{[L_{\text{ini}},L-1]}. \end{array} \right\} \tag{9}$$

Note that in (9) we consider the initial condition $Z_{0|k} = \sum_{j=0}^{L-1} \mathsf{z}^j_{0|k}\phi^j$ to be a random variable rather than the current realization z_k. Specifically, as $\mu \in [0,1]$ we enforce the expected value (the PCE coefficients with $j = 0$) and the covariance of $Z_{0|k}$ to be a convex combination of z_k and $Z^\star_{1|k-1} = \sum_{j=0}^{L-1} \mathsf{z}^{j,\star}_{1|k-1}\phi^j$ which is the predicted valued of Z_k. In addition, we can design the distribution of $Z_{0|k}$ by the choice of $\{\phi^j_{\text{ini}}\}_{j=0}^{L_{\text{ini}}-1}$ which is equivalent to $\{\phi^j\}_{j=0}^{L_{\text{ini}}-1}$ as shown in (6). For the sake of efficient computation, we consider $\{\phi^j_{\text{ini}}\}_{j=1}^{L_{\text{ini}}-1}$ to be n_z dimensional i.i.d. Gaussian,

$$\phi^0_{\text{ini}} = 1, \quad L_{\text{ini}} = n_z + 1, \quad \phi^j_{\text{ini}} \sim \mathcal{N}(0,1), \quad \forall j \in \mathbb{I}_{[1,n_z]}. \tag{10}$$

This way, we have $Z_{0|k}$ also to be Gaussian since it is a linear combination of $\{\phi^j_{\text{ini}}\}_{j=0}^{L_{\text{ini}}-1}$. Notice that this choice does not prevent the consideration of non-Gaussian disturbances since the basis φ^j for disturbances in (6) is chosen according to the underlying distribution.

Moreover, with $\{\phi^j_{\text{ini}}\}_{j=0}^{L_{\text{ini}}-1}$ satisfying (10), we reformulate the quadratic and nonconvex equality constraints of (9) in a linear fashion. Specifically, note that the right-hand-side matrix of the quadratic equality constraint $Q_{\text{rhs}} \doteq \sum_{j=1}^{L-1} \mathsf{z}^{j,\star}_{1|k-1}\mathsf{z}^{j,\star\top}_{1|k-1}\|\phi^j\|^2 = Q^\top_{\text{rhs}} \succeq 0$ is known prior to solving the OCP. Hence, we can compute its eigen-decomposition $Q_{\text{rhs}} = U_{\text{rhs}}\, D_{\text{rhs}}U^\top_{\text{rhs}}$, where D_{rhs} is a diagonal matrix with non-negative elements. Then, one positive semi-definite solution of the non-convex quadratic equality constraint reads

$$[\mathsf{z}^1_{0|k}, \mathsf{z}^2_{0|k}, \ldots, \mathsf{z}^{n_z}_{0|k}] = (1-\mu)U_{\text{rhs}}D^{\frac{1}{2}}_{\text{rhs}}U^\top_{\text{rhs}}, \tag{11}$$

since $\|\phi^j\|^2 = \|\phi^j_{\text{ini}}\|^2 = 1$ holds for $j \in \mathbb{I}_{[1,n_z]}$ if (10) is considered. Substituting the second constraint of (9) by (11), we avoid the non-convexity at the cost of computing one small-scale eigen-decomposition prior to each optimization. This reformulation may cause performance loss since it replaces the original quadratic equality with one specific feasible solution.

3.2. Predictive control scheme and closed-loop properties

With the interpolated initial conditions, we extend the output-feedback stochastic data-driven predictive control scheme proposed by Pan et al. (2022a) based on OCP (8).

The predictive control scheme consists of an off-line data collection phase and an on-line optimization phase. In the off-line phase, a random input and disturbance trajectory $(\mathbf{u}, \mathbf{w})_{[0,T-1]}$ is generated to obtain $\mathbf{y}_{[0,T-1]}$. Note that the disturbance trajectory $\mathbf{w}_{[0,T-1]}$ can also be estimated from output data, cf. (Pan et al., 2022b; Wang et al., 2022b) for details. Moreover, the recorded input, output, and disturbance trajectories are used to determine the terminal ingredients and to construct the Hankel matrices for OCP (8).

In the on-line optimization phase, we assume the OCP (8) is feasible at time instant $k = 0$ with $\mathsf{z}^{0,\star}_{1|-1} = z_0, \mathsf{z}^{j,\star}_{1|-1} = 0$, $j \in \mathbb{I}_{[1,L-1]}$ in (8c) such that only the measured initial condition z_0 is considered. Then at each time k, we solve OCP (8) to obtain the PCE coefficients of the first optimal input and the interpolated initial condition, i.e. $\mathsf{u}^{j,\star}_{0|k}$ and $\mathsf{z}^{j,\star}_{0|k}$, respectively. Notice that $\mathsf{u}^{j,\star}_{0|k} = 0$ holds for $j \in \mathbb{I}_{[L_{\text{ini}},L-1]}$ due to the causality condition (8e). Specifically, we consider the feedback input u^{cl}_k as a realization of random variable given by $\mathsf{u}^{j,\star}_{0|k}$, that is $u^{\text{cl}}_k = \sum_{j=0}^{L_{\text{ini}}-1} \mathsf{u}^{j,\star}_{0|k}\phi^j_{\text{ini}}(\omega)$, where $\{\phi^j_{\text{ini}}(\omega)\}_{j=1}^{L_{\text{ini}}-1}$ are obtained by considering the the current measured z_k as a realization of random variable given by $\mathsf{z}^{j,\star}_{0|k}$, cf. (Pan et al., 2022a). With the basis for the initial condition as specified in (10), $u^{\text{cl}}_k = \sum_{j=0}^{L_{\text{ini}}-1} \mathsf{u}^{j,\star}_{0|k}\phi^j_{\text{ini}}(\omega)$ then is a linear system of equations. Finally, the optimal solution to OCP (8) is indeed an affine feedback policy in the realizations $\phi^j_{\text{ini}}(\omega)$.

Applying the feedback input u_k^{cl} determined from above, the closed-loop dynamics of (2) for a given initial condition $z_{\text{ini}}^{\text{cl}}$ and disturbances $\{w_k\}_{k\in\mathbb{N}}$ read

$$y_k^{\text{cl}} = \Phi z_k^{\text{cl}} + D u_k^{\text{cl}} + w_k, \quad z_0^{\text{cl}} = z_{\text{ini}}^{\text{cl}}. \tag{12a}$$

Moreover, we obtain the sequence $V_{N,k} \in \mathbb{R}$, $k \in \mathbb{N}$ corresponding to the optimal value function of (8) evaluated in the closed loop. Accordingly, considering a probabilistic initial condition $Z_{\text{ini}}^{\text{cl}}$ and probabilistic disturbance W_k, $k \in \mathbb{N}$, we obtain the closed-loop dynamics in random variables

$$Y_k^{\text{cl}} = \Phi Z_k^{\text{cl}} + D U_k^{\text{cl}} + W_k, \quad Z_0^{\text{cl}} = Z_{\text{ini}}^{\text{cl}}, \tag{12b}$$

where conceptually the realization of U_k^{cl} is u_k^{cl}. Similarly, we define the probabilistic optimal cost $\mathcal{V}_{N,k} \in \mathcal{L}^2(\Omega, \mathcal{F}, \mu; \mathbb{R})$ as $\mathcal{V}_{N,k}(\omega) = V_{N,k}$. The following theorem summarizes the closed-loop properties of the proposed scheme.

Theorem 4 (Recursive feasibility and asymptotic average cost bound) *Consider the closed-loop dynamics (12) resulting from the proposed predictive control algorithm based on OCP (8). Let Assumptions 1–2 hold. Suppose that at time instant $k = 0$, OCP (8) is feasible with the initial condition in (8c) as $\mathsf{z}_{1|-1}^{0,\star} = z_0^{cl} = z_{ini}^{cl}$, $\mathsf{z}_{1|-1}^{j,\star} = 0, j \in \mathbb{I}_{[1,L-1]}$. Then, OCP (8) is feasible at all time instants $k \in \mathbb{N}^+$ with the initial condition in (8c) updated with the current measured initial condition z_k^{cl} and the predicted PCE coefficients $\mathsf{z}_{1|k-1}^{\star}$ based on the optimal solution of the previous solution obtained at $k-1$.*

Moreover, let $\alpha \doteq \operatorname{trace}\left(\Sigma_W(Q + \widetilde{E}^\top P \widetilde{E})\right) \in \mathbb{R}^+$, then the following statements hold:

(i) The optimal performance index of OCP (8) at consecutive time instants satisfies $\mathbb{E}\left[\mathcal{V}_{N,k+1} - \mathcal{V}_{N,k}\right] \leq -\mathbb{E}\left[\|U_k^{cl}\|_R^2 + \|Y_k^{cl}\|_Q^2\right] + \alpha$.

(ii) In addition, $\lim_{k\to\infty} \frac{1}{k}\sum_{i=0}^{k} \mathbb{E}\left[\|U_i^{cl}\|_R^2 + \|Y_i^{cl}\|_Q^2\right] \leq \alpha$, *i.e., the asymptotic average cost of the proposed algorithm is bounded from above by α.*

Proof (Sketch) In Pan et al. (2022a), we present sufficient conditions for recursive feasibility and the asymptotic average cost bound of the aforementioned predictive scheme with binary selection of initial condition, i.e. $\mu \in \{0, 1\}$. The proof relies on the fact that with $\mu = 1$ OCP (8) is recursively feasible, cf. (Pan et al., 2022a, Proposition 1). Hence, with the interpolation condition (9), i.e. $\mu \in [0, 1]$, the recursive feasibility naturally holds since $\mu = 1$ is included. Moreover, due to the optimization over the initial condition, the optimal cost $V_{N,k}$ with $\mu \in [0, 1]$ is bounded from above by the one with $\mu \in \{0, 1\}$, which allows to infer the bound for the asymptotic average cost via the proof of (Pan et al., 2022a, Theorem 1). ■

4. Numerical Example

We consider the LTI aircraft model given by Maciejowski (2002) exactly discretized with sampling time $t_s = 0.5$ s. The system matrices are

$$\Phi = \begin{bmatrix} -0.019 & -1.440 & -0.201 & 0.256 & 0.050 & 0.160 & -0.256 & 0.0860 \\ 0.711 & -1.800 & -4.773 & 3.6875 & 0.650 & 2.982 & -2.688 & 1.707 \\ 1.444 & -26.922 & -15.746 & 12.898 & 2.319 & 10.461 & -12.897 & 5.171 \end{bmatrix},$$

and $D = 0_{3\times 1}$ with $n_y = 3$, $n_u = 1$, $T_{\text{ini}} = 2$, and thus $n_z = 8$. Its minimal state-space representation with $n_x = 4$ can be found in (Pan et al., 2022b). As the simulated plant, we consider the system dynamics (1), where $W_k, k \in \mathbb{N}$ are i.i.d. uniform random variables with their support on $[-0.01, 0.01] \times [-1, 1] \times [-0.1, 0.1]$. Note that Y^j denotes the j-th element of Y. We impose a chance constraint on Y^1, i.e. $\mathbb{P}[Y^1 \in \mathbb{Y}^1] \geq 1 - \varepsilon_y$, where $\mathbb{Y}^1 = [-1, 1]$, $\varepsilon_y = 0.1$, and $\sigma(\varepsilon_y) = \sqrt{(2-\varepsilon_y)/\varepsilon_y} = 4.359$. The weighting matrices are $Q = \text{diag}([1, 1, 1])$ and $R = 1$.

We apply the proposed scheme with prediction horizon $N = 10$. In the data collection phase we record input-output trajectories of 90 steps to construct the Hankel matrices and to determine terminal ingredients P, Γ, γ and $\mathbb{Z}_\text{f}$, cf. (Pan et al., 2022a). To obtain an exact PCE for each component of W_k, we employ Legendre polynomials component-wisely such that $L_w = 4$. As shown in (10), we choose the basis for initial condition accordingly with $L_{\text{ini}} = 1 + n_z = 9$. Thus, from (6), the dimension of the overall PCE basis as $L = 39$.

With 50 different sampled sequences of disturbance realizations, we show the corresponding closed-loop realization trajectories of the proposed scheme in the left top of Figure 1. It can be seen that the chance constraint for output Y^1 is satisfied with a high probability, while Y^2 and Y^3 converged to a neighborhood of 0. The averaged-in-time cost trajectories are depicted in the left bottom of Figure 1 in a semi-logarithmic plot. We see the sampled averaged asymptotic value is 251.0 and is bounded from above by $\alpha = 295.21$. This is in line with the insights of Theorem 4. To illustrate the evolution of statistical distributions of the closed-loop trajectories (12b), we sample a total of 1000 sequences of disturbance realizations and initial conditions around $[0, -100, 0]^\top$. Then, we compute the corresponding closed-loop responses. The time evolution of the normalized histograms of the output realizations y^2 at $k = 0, 5, 10, 15, 20$ is depicted in the right of Figure 1, where the vertical axis can be regarded as the approximated probability density of Y^2. As one can see, the proposed control scheme controls the system to a narrow distribution for Y^2 centred at 0.

Furthermore, we compare the proposed scheme with the interpolation of initial conditions to the binary selection in Pan et al. (2022a). This is done by evaluating the 50-steps closed-loop system responses for both schemes with the same closed-loop initial condition $z^{\text{cl}}_{\text{ini}}$ and the same disturbance sequence $\{w_k\}_{k\in\mathbb{N}}$. The binary selection scheme takes about $100.68\,\text{s}$ to evaluate, while the proposed interpolation scheme takes $54.44\,\text{s}$. The reason for this performance difference lies in the fact that the binary scheme occasionally needs to solve two OCPs. More precisely, the binary scheme solves two OCPs 28 times in the 50 time steps that is about 60% of the whole closed-loop steps. As shown in Figure 2, the system responses are almost identical for the two schemes with the maximal input difference of $4.29 \cdot 10^{-8}\,\text{rad}$. The evolution of the interpolation scalar μ is depicted in the last plot of Figure 2.

5. Conclusion

This paper has investigated data-driven stochastic output-feedback predictive control of linear time-invariant systems. We have shown that the concept of interpolating initial conditions can and should be exploited in the data-driven stochastic setting. Specifically, we have given sufficient conditions for recursive feasibility and practical stability as well as a corresponding performance bound. Numerical results illustrate the efficacy of the proposed approach. Our results, which are based on a recently proposed stochastic extension to Willems' fundamental lemma, underpin that stochastic predictive control can be formulated in data-driven fashion. Future work will consider tailored numerical methods for real-time feasible implementation and less restrictive stability conditions.

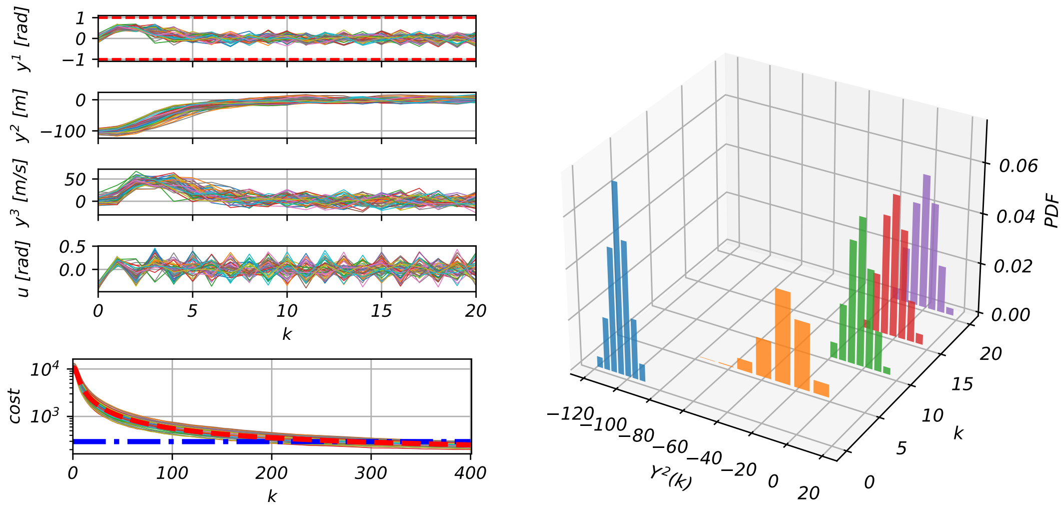

Figure 1: (Left-top) 50 different closed-loop realization trajectories. The red-dashed lines show the chance constraints. (Left-bottom) Averaged cost (over time) of 50 different closed-loop realization trajectories. The red dashed lines depict the averaged asymptotic cost over samplings; the blue dash-dotted line denotes the bound α as in Theorem 4. (Right) Histograms of the output Y^2 from 1000 closed-loop realization trajectories.

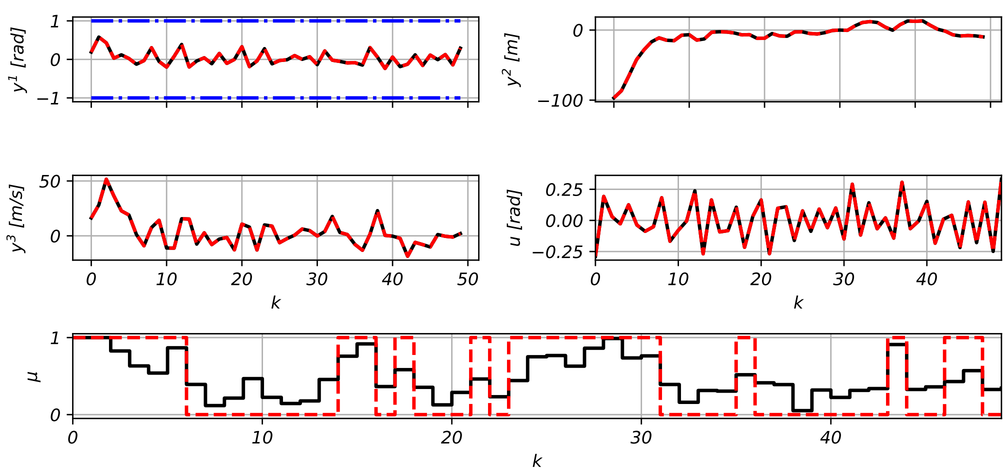

Figure 2: Comparison of system responses for schemes with the interpolation or the binary selection of the initial conditions. The black line denotes the system response of the interpolation scheme; the red dashed line denotes the system response of the binary scheme.

Acknowledgments

The authors gratefully acknowledge funding by the German Research Foundation (Deutsche Forschungsgemeinschaft DFG) under project number 499435839.

References

Ahmed Allibhoy and Jorge Cortes. Data-driven distributed predictive control via network optimization. In *Proceedings of the 2nd Conference on Learning for Dynamics and Control*, volume 120 of *Proceedings of Machine Learning Research*, pages 838–839. PMLR, 10–11 Jun 2020.

Julian Berberich, Johannes Köhler, Matthias A. Müller, and Frank Allgöwer. Data-driven model predictive control with stability and robustness guarantees. *IEEE Transactions on Automatic Control*, 66(4):1702–1717, 2020.

Julian Berberich, Johannes Köhler, Matthias A. Müller, and Frank Allgöwer. On the design of terminal ingredients for data-driven MPC. *IFAC-PapersOnLine*, 54(6):257–263, 2021.

Deborah Bilgic, Alexander Koch, Guanru Pan, and Timm Faulwasser. Toward data-driven predictive control of multi-energy distribution systems. *Electric Power Systems Research*, 212:108311, 2022.

Joscha Bongard, Julian Berberich, Johannes Köhler, and Frank Allgöwer. Robust stability analysis of a simple data-driven model predictive control approach. *IEEE Transactions on Automatic Control*, 68(5):2625–2637, 2023. doi: 10.1109/TAC.2022.3163110.

Paolo Gherardo Carlet, Andrea Favato, Riccardo Torchio, Francesco Toso, Saverio Bolognani, and Florian Dörfler. Real-time feasibility of data-driven predictive control for synchronous motor drives. *IEEE Transactions on Power Electronics*, 38(2):1672–1682, 2023. doi: 10.1109/TPEL.2022.3214760.

Jeremy Coulson, John Lygeros, and Florian Dörfler. Data-enabled predictive control: In the shallows of the DeePC. In *2019 18th European Control Conference (ECC)*, pages 307–312. IEEE, 2019.

Claudio De Persis and Pietro Tesi. Formulas for data-driven control: Stabilization, optimality, and robustness. *IEEE Transactions on Automatic Control*, 65(3):909–924, 2020. doi: 10.1109/TAC.2019.2959924.

Marcello Farina, Luca Giulioni, Lalo Magni, and Riccardo Scattolini. A probabilistic approach to model predictive control. In *52nd IEEE Conference on Decision and Control*, pages 7734–7739, 2013. doi: 10.1109/CDC.2013.6761117.

Marcello Farina, Luca Giulioni, Lalo Magni, and Riccardo Scattolini. An approach to output-feedback MPC of stochastic linear discrete-time systems. *Automatica*, 55:140–149, 2015.

Timm Faulwasser, Ruchuan Ou, Guanru Pan, Philipp Schmitz, and Karl Worthmann. Behavioral theory for stochastic systems? A data-driven journey from Willems to Wiener and back again. *Annual Reviews in Control*, 2023. ISSN 1367-5788. doi: https://doi.org/10.1016/j.arcontrol.2023.03.005.

N. Kantas, J. M. Maciejowski, and A. Lecchini-Visintini. *Sequential Monte Carlo for model predictive control*, pages 263–273. Springer Berlin Heidelberg, Berlin, Heidelberg, 2009. ISBN 978-3-642-01094-1. doi: 10.1007/978-3-642-01094-1_21.

Sebastian Kerz, Johannes Teutsch, Tim Brüdigam, Dirk Wollherr, and Marion Leibold. Data-driven stochastic model predictive control. *arXiv preprint arXiv:2112.04439*, 2021.

Roelof Koekoek and René F. Swarttouw. The Askey-scheme of hypergeometric orthogonal polynomials and its q-analogue. Technical Report 98-17, Department of Technical Mathematics and Informatics, Delft University of Technology, Delft, The Netherlands, 1998.

Johannes Köhler and Melanie N. Zeilinger. Recursively feasible stochastic predictive control using an interpolating initial state constraint. *IEEE Control Systems Letters*, 2022.

Milan Korda, Ravi Gondhalekar, Jiří Cigler, and Frauke Oldewurtel. Strongly feasible stochastic model predictive control. In *2011 50th IEEE Conference on Decision and Control and European Control Conference*, pages 1245–1251. IEEE, 2011.

Tom Lefebvre. On moment estimation from polynomial chaos expansion models. *IEEE Control Systems Letters*, 5(5):1519–1524, 2021. doi: 10.1109/LCSYS.2020.3040851.

Yingzhao Lian and Colin N. Jones. Nonlinear data-enabled prediction and control. In *Proceedings of the 3rd Conference on Learning for Dynamics and Control*, volume 144 of *Proceedings of Machine Learning Research*, pages 523–534. PMLR, 07 – 08 June 2021.

J. M. Maciejowski. *Predictive Control with Constraints*. Pearson Education, 2002.

Ivan Markovsky and Florian Dörfler. Behavioral systems theory in data-driven analysis, signal processing, and control. *Annual Reviews in Control*, 52:42–64, 2021. ISSN 1367-5788.

Ali Mesbah, Stefan Streif, Rolf Findeisen, and Richard D. Braatz. Stochastic nonlinear model predictive control with probabilistic constraints. In *2014 American Control Conference*, pages 2413–2419, 2014. doi: 10.1109/ACC.2014.6858851.

Tillmann Mühlpfordt, Rolf Findeisen, Veit Hagenmeyer, and Timm Faulwasser. Comments on truncation errors for polynomial chaos expansions. *IEEE Control Systems Letters*, 2(1):169–174, 2018. doi: 10.1109/LCSYS.2017.2778138.

Ruchuan Ou, Michael Heinrich Baumann, Lars Grüne, and Timm Faulwasser. A simulation study on turnpikes in stochastic LQ optimal control. *IFAC-PapersOnLine*, 54(3):516–521, 2021. doi: https://doi.org/10.1016/j.ifacol.2021.08.294. 16th IFAC Symposium on Advanced Control of Chemical Processes ADCHEM 2021.

Guanru Pan, Ruchuan Ou, and Timm Faulwasser. On data-driven stochastic output-feedback predictive control. *arXiv preprint arXiv:2211.17074*, 2022a.

Guanru Pan, Ruchuan Ou, and Timm Faulwasser. On a stochastic fundamental lemma and its use for data-driven optimal control. *IEEE Transactions on Automatic Control*, pages 1–16, 2022b. doi: 10.1109/TAC.2022.3232442.

Guanru Pan, Ruchuan Ou, and Timm Faulwasser. Towards data-driven stochastic predictive control. *International Journal of Robust and Nonlinear Control*, 2022c. Submitted.

Joel A. Paulson, Ali Mesbah, Stefan Streif, Rolf Findeisen, and Richard D. Braatz. Fast stochastic model predictive control of high-dimensional systems. In *53rd IEEE Conference on Decision and Control*, pages 2802–2809, 2014. doi: 10.1109/CDC.2014.7039819.

Tomonori Sadamoto. On equivalence of data informativity for identification and data-driven control of partially observable systems. *IEEE Transactions on Automatic Control*, pages 1–8, 2022. doi: 10.1109/TAC.2022.3202082.

Georg Schildbach, Lorenzo Fagiano, Christoph Frei, and Manfred Morari. The scenario approach for stochastic model predictive control with bounds on closed-loop constraint violations. *Automatica*, 50(12):3009–3018, 2014. ISSN 0005-1098.

Henning Schlüter and Frank Allgöwer. Stochastic model predictive control using initial state optimization. *IFAC-PapersOnLine*, 55(30):454–459, 2022. ISSN 2405-8963. doi: https://doi.org/10.1016/j.ifacol.2022.11.095. 25th International Symposium on Mathematical Theory of Networks and Systems MTNS 2022.

Tim J. Sullivan. *Introduction to Uncertainty Quantification*, volume 63. Springer, 2015.

Roberto Tempo, Giuseppe Calafiore, and Fabrizio Dabbene. *Randomized algorithms for analysis and control of uncertain systems: with applications*. Springer London, 2 edition, 2013.

Jiawei Wang, Yang Zheng, Keqiang Li, and Qing Xu. DeeP-LCC: Data-enabled predictive leading cruise control in mixed traffic flow. *arXiv preprint arXiv:2203.10639*, 2022a.

Yibo Wang, Chao Shang, and Dexian Huang. Data-driven control of stochastic systems: An innovation estimation approach. *arXiv preprint arXiv:2209.08995*, 2022b.

Norbert Wiener. The homogeneous chaos. *American Journal of Mathematics*, pages 897–936, 1938.

Jan C. Willems, Paolo Rapisarda, Ivan Markovsky, and Bart L.M. De Moor. A note on persistency of excitation. *Systems & Control Letters*, 54(4):325–329, 2005. doi: https://doi.org/10.1016/j.sysconle.2004.09.003.

Liang Wu. Equivalence of SS-based MPC and ARX-based MPC. *arXiv preprint arXiv:2209.00107*, 2022.

Dongbin Xiu and George Em Karniadakis. The Wiener–Askey polynomial chaos for stochastic differential equations. *SIAM Journal on Scientific Computing*, 24(2):619–644, 2002. doi: 10.1137/S1064827501387826.

Hua Yang and Shaoyuan Li. A data-driven predictive controller design based on reduced Hankel matrix. In *2015 10th Asian Control Conference (ASCC)*, pages 1–7, 2015. doi: 10.1109/ASCC.2015.7244723.